IOPscience iopscience.iop.org

Home Search Collections Journals About Contact us My IOPscience

The temperature dependence of current–voltage characteristics of the Au/Polypyrrole/p-Si/Al heterojunctions

This article has been downloaded from IOPscience. Please scroll down to see the full text article.

2006 J. Phys.: Condens. Matter 18 2665

(http://iopscience.iop.org/0953-8984/18/9/006)

View the table of contents for this issue, or go to the journal homepage for more

Download details:
IP Address: 129.252.86.83
The article was downloaded on 28/05/2010 at 09:02

Please note that terms and conditions apply.

Institute of Physics Publishing — Journal of Physics: Condensed Matter
J. Phys.: Condens. Matter **18** (2006) 2665–2676 doi:10.1088/0953-8984/18/9/006

The temperature dependence of current–voltage characteristics of the Au/Polypyrrole/p-Si/Al heterojunctions

Ş Aydoğan, M Sağlam and A Türüt

Department of Physics, Faculty of Sciences and Arts, Atatürk University, 25240 Erzurum, Turkey

Received 4 July 2005, in final form 28 December 2005
Published 17 February 2006
Online at stacks.iop.org/JPhysCM/18/2665

Abstract
The current–voltage (I–V) characteristics of Au/Polypyrrole/p-Si/Al contacts have been measured at temperatures ranging from 70 to 280 K. The I–V characteristics of the device have rectifying behaviour with a potential formed at the interface. The high values of the ideality factor n depending on the sample temperature may be ascribed to a decrease of the exponentially increasing rate in current due to space-charge injection into the PPy thin film at higher forward bias voltage. The experimental reverse bias I–V characteristics of the device followed the Schottky-like conduction model or Poole–Frenkel effect formulae. A linear temperature dependence of the barrier height Φ_b from the reverse bias I–V characteristics was observed, and the Φ_{bo} value decreased with lowering temperature, ranging from 0.69 eV at 280 K to 0.22 eV at 70 K.

1. Introduction

In recent years, conducting polymers [1–5] and organic semiconducting films [6–8] have been the subject of great interest to chemists and physicists. Polypyrrole (PPy) has been one of the most studied polymers because of its physical and electrical properties, excellent environment stability, and ease of preparation either by chemical or electrochemical polymerization that have led to several applications such as solid state devices and electronics [9–13]. Generally, the junctions between p-Si and metals with high work functions such as gold or aluminium are expected to form an ohmic contact. Therefore, so far many attempts have been made to realize the formation of a rectifying contact or modification of the barrier height or the continuous control of the barrier height using an organic semiconductor layer [5–12] or an insulating layer and a chemical passivation procedure [21–29] at certain metal/inorganic semiconductor interfaces, or to determine the characteristic parameters of organic films [5–12]. In the passivation process case, inorganic/organic semiconductor diodes may be sensitive probes that are useful for increasing the quality of devices fabricated using an organic semiconductor in establishing processes for minimizing surface states, surface damage and contamination. Such studies not only make inorganic semiconductor/organic film interfaces potentially relevant in

 © 2006 IOP Publishing Ltd Printed in the UK

the fabrication of Schottky type diodes with well-defined or actively tunable barrier heights, but also in the fundamental study of electronic processes at semiconductor interfaces.

Nguyen and Kamloth [10–12] have prepared a conducting organic polymer (electrochemically polymerized PPy) using tetraethylammonium toluenesulfonate (TOS), nickel or copper phthalocyanine toluenesulfonate (NiPcTS), (CuPcTS) as dopant, and calculated the junction parameters of Au/doped PPy layer contacts from its current–voltage (I–V) and capacitance–voltage (C–V) characteristics; and they have shown that these junctions exhibit a significant, fast and reversible response to nitrogen oxide gas (NO_x) which was explained by changes in the Schottky barrier height and in the carrier concentration of the PPy layer due to NO_x exposure. Furthermore, they [12] have studied the influence of thickness and preparation temperature of doped PPy films on the electrical and chemical sensing properties of these junctions. Nitrogen oxide, NO_2 or (NO_x) sensing has been also investigated by some groups using different organic films [30–32]. It was found that NO_x exhibits strong acceptor behaviour. Therefore, interaction of NO_x with a p-type polymer layer enhances the doping level. In this case, a low Schottky barrier may be formed at the junction between a highly doped p-type polymer and a metal with high work function, e.g. gold [10–12]. Some researchers [14–18] have studied the electronic properties of the polymer/PPy [14, 15] and PPy/inorganic semiconductor [16–18] heterostructures from their I–V, C–V and conductivity–temperature characteristics. Some activities have been also focused on understanding and controlling key parameters such as the interface potential barriers [16–27]. Thicker organic interlayers of the conjugated molecules have also been successfully used to modify effective barriers [16–20]. Dakhel [27] have prepared thin Nd oxide films on p-Si substrates to form MOS structures (Al/Nd_2O_3/Si/Al structures) being annealed at different conditions. He [27] has showed that the carrier transport through the device follows the space charge limited current (SCLC) mechanism described by exponential or uniform distribution of localized levels in the band gap, depending on the annealing conditions of the oxide.

We have studied the forward and reverse bias current–voltage (I–V) characteristics of Au/PPy/p-Si/Al heterojunction structures in the temperature range 70–280 K. The PPy layer on p-Si substrate was fabricated from the electrolyte solution being held at a constant temperature of 55 °C. Al was evaporated on the back surface of the p-type Si substrate for ohmic contact, and Au was evaporated on the surface of the PPy for the circular pseudo-Schottky contact. As indicated above, electronic devices invariably rely on the properties of interfaces between electrical conductors. Examples abound from devices such as batteries, solar cells, light emitting diodes, transistors, and sensors; and it is expected that conducting polymers exhibiting semiconducting properties are an excellent candidate material for electron devices. Therefore, the successful application of conjugated polymers to such devices requires an understanding of charge transport at their interfaces and bulk parameters [3, 10–19, 33]. Likewise, the primary purpose of this paper is to explain the behaviour of the experimental forward and reverse I–V–T characteristics of the heterojunction at the intermediate and high bias voltage regions using the exiting electrical conduction models to determine the predominant charge transport mechanism for this device.

PPy/p-Si is not a novel and unique device. We have previously published a series of papers concerning conducting polymer/Si (p or n) structures [16], for example: the I–V characteristics of Sn/PPy/n-Si and Polyaniline/p-Si/Al structures in the temperature range 90–300 K have shown a Gaussian distribution behaviour of the barrier heights due to barrier height inhomogeneity [16], and moreover it has been seen that the forward and reverse bias I–V characteristics of PPy/p-InP at room temperature have shown Schottky diode behaviour [16]. As will be discussed later, the double-logarithmic forward bias I–V characteristics of the considered Au/PPy/p-Si structure here have shown a power-law behaviour of the current

$I \propto V^{m+1}$ with different exponents $(m + 1)$ in contrast to the I–V characteristics of our devices in [16]. Moreover, Si wafers were used as electrode or substrate for fabrication of the organic (PPy) diodes also in [2, 17, 33]. The I–V characteristics of these devices [2, 17, 33] were only interpreted by the thermionic current model and at room temperature in contrast to our study.

2. Experimental procedure

A polished p-type Si wafer with (100) orientation and 5–10 Ω cm resistivity was used as substrate and chemically cleaned by the RCA cleaning procedure (i.e., a 10 min boil in $NH_3 + H_2O_2 + 6H_2O$ followed by a 10 min boil in $HCl + H_2O_2 + 6H_2O$). The native oxide on the front surface of the Si was removed in $HF:H_2O$ (1:10) solution, and finally the wafer was rinsed in de-ionized water for 30 s before forming the organic layer on the p-type Si substrate The native oxide on the front surface of the Si substrate was removed in $HF:H_2O$ (1:10) solution and finally the wafer was rinsed in de-ionized water for 30 s. Aluminium was evaporated on the back surface of the p-type Si substrate to make ohmic contact, followed by a temperature treatment at 570 °C for 3 min in N_2 atmosphere before the anodization process. The ohmic contact side of the Si substrate used as an anode and its edges were carefully covered by black wax, and then the polished and cleaned front side of the sample was exposed to the electrolyte by mounting it on an experimental setup employed for anodization. A Pt plate was used as cathode in the experimental setup. The polymer film was electrochemically deposited on the surface of the semiconductor (p-Si) under a constant current density of 4 mA cm^{-2}. The PPy film on the front surface of the p-type Si substrate was obtained from the electrolyte solution being held at a constant temperature of 55 °C. The electrolyte was composed of 0.40 M pyrrole and 0.10 M tetrabutylammonium tetrafluoroborate. The purified pyrrole was obtained from Fluka Chimika and it was used to prepare polypyrrole (PPy) at room temperature. The electrolyte solution was prepared in a propylene carbonate solvent (Merck trademark). Finally, the Au top metal was evaporated through a shadow mask on the PPy surface to obtain an Au/PPy/p-Si/Al structure. The area of circular Schottky contacts was 2.27×10^{-2} cm^2. All metallic surfaces were cleaned with acetone and methanol before the processes. All evaporation processes were carried out in a turbo molecular fitted vacuum coating unit at about 10^{-5} Torr. The I–V characteristics of the devices were measured in the temperature range 70–280 K using a Leybold Heraeus closed-cycle helium cryostat that enables us to make measurements in the temperature range 10–340 K, and a Keithley 487 picoammeter/voltage source in dark conditions. The sample temperature was always monitored by a copper–constantan thermocouple and a Windaus MD850 electronic thermometer with sensitivity better than ±0.1 K.

3. Results and discussion

Figure 1 shows the experimental semi-logarithmic forward and reverse bias current–voltage (I–V) characteristics of the Au/PPy/p-Si/Al heterojunction in the temperature range 70–280 K. In the forward bias case of the device, the Al electrode (ohmic contact) was positively biased with respect to the Au electrode (Schottky contact) on the PPy layer. First, let us treat the experimental I–V data using an empirical relation of the form $I(V, T) \propto \exp(eV/nkT)$ that is known as the thermionic emission current mechanism for transport across the rectifying junction. The values of the ideality diode factor n from the slopes of the linear portions of the semi-log forward bias I–V characteristics were calculated in the range 2.229 (at 280 K) to 5.768 (at 70 K), depending on the actual conduction processes in the junction. The ideality

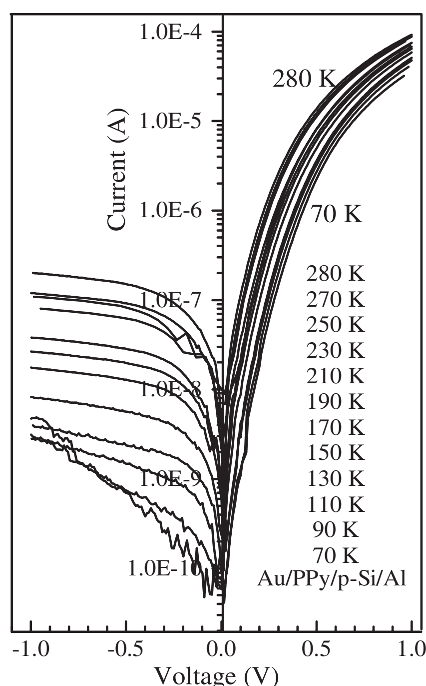

Figure 1. Experimental forward and reverse bias current–voltage characteristics of a typical Au/PPy/p-Si/Al hetero-contact in the temperature range 70–280 K.

factor n is a measure of conformity of the diode to pure thermionic emission. The very strong temperature dependence of the ideality factor shows that the forward bias transport properties of the present device at intermediate and high bias voltage are not well modelled only by the thermionic emission even when it was modified by the incorporation of a series resistance effect. This suggests that the current processes occurring in the highly resistive PPy layer of the Au/PPy/p-Si/Al heterojunction would be a possible alternative candidate in determining the forward current at the intermediate and high bias regimes beyond that of the low bias diode-like behaviour.

The doping level of the PPy layer decreases with the increase of the PPy layer thickness as reported in [9]. The PPy layer thickness is about 210 nm. Furthermore, the concentration of the active charge carriers is dependent on the preparation temperature and decreases with increasing preparation temperature [10, 28]. We prepared the PPy layer on the p-Si substrate from the electrolyte solution at a constant temperature of 55 °C. On the other hand, as can be seen from figure 1, a slight saturating behaviour is observed in the reverse bias because the junction-like conduction processes occurring in depletion region should limit the measured heterojunction reverse current. The experimental reverse bias I–V characteristics of the device mentions that the appropriate rectifying junction-like formulae (such as the Schottky-like conduction model) can be applied to examine its reverse bias I–V plots in the reverse bias case, that is, a rectifying junction-like behaviour should be dominant [29].

Figures 2(a) and (b) show the forward and reverse bias $\ln I$ as a function of the sample temperature of the heterojunction device, respectively, in the voltage range 0.20–1.00 V with steps of 0.02 V. In figure 2(a), the open triangles represent the experimental forward bias case and the solid lines represent the fit to experimental data; in figure 2(b), the continuous curves

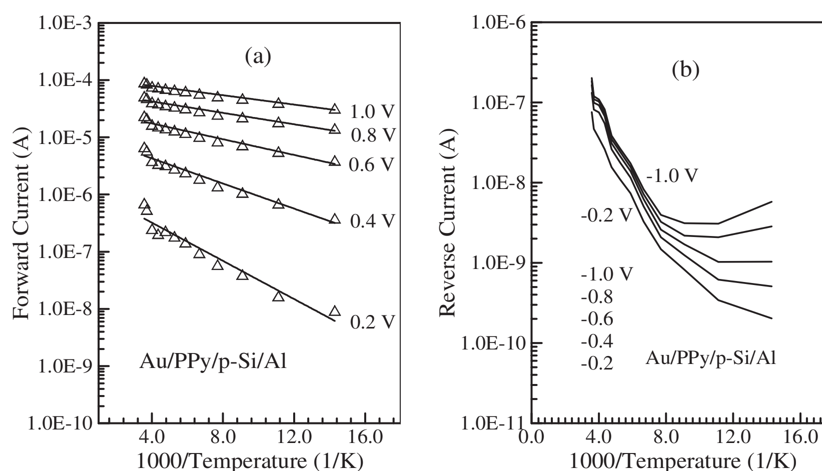

Figure 2. The $\ln(I)$ versus $1/T$ plot of the Au/PPy/p-Si/Al hetero-contact at five different voltages from figure 1 in the temperature range 70–280 K. (a) The experimental forward bias case (the open triangles); the solid lines represent the fit to experimental data, (b) the continuous curves represent the experimental reverse bias case.

represent the experimental reverse bias case. These Arrhenius or Richardson curves should give a straight line. The forward $\ln I$–$1/T$ curves (figure 2(a)) exhibit linear behaviour in the temperature range 70–280 K and the slope of the straight lines decreases with increasing bias voltage. The reverse bias $\ln I$–$1/T$ curves (figure 2(b)) only exhibit a bias-independent linearity in the temperature range 110–280 K. The reverse bias curves deviate from the Arrhenius or Richardson linearity with decreasing temperature in the temperature range 110–70 K, and the deviation increases with increasing voltage in this temperature range. This implies that the high bias conduction processes in the reverse bias differ from those giving rise to the high bias forward current behaviour. Assuming that the junction depletion region still limits the device electrical behaviour, the experimentally observed deviation of its forward-current behaviour at high bias voltages from the I–V characteristics of a diode-like junction in the low bias voltage can be explained in terms of a series-resistance effect, which may remarkably modify the actual rectifying junction-like behaviour at high bias voltages. An ohmic voltage term IR_s is usually included in the diode-like formula to account for such a series-resistance effect [19, 29, 40, 41]. Therefore, the effect of bulk conduction in a device having a highly resistive semiconducting layer becomes important in a junction at high bias voltages in the forward bias direction and not in the reverse bias case where a rectifying junction-like behaviour should be dominant [29, 40, 41]. Likewise, figures 1 and 2 show that the forward and reverse bias I–V–T characteristics of the present heterojunction are dissimilar, at least in two major respects as determined in [29]. First, the reverse current levels are much lower than the forward current values at the same ambient temperature and bias voltage as can be seen in figure 1. Second, the behaviour of the reverse current with temperature and bias voltage in the high bias region is seemingly of different conduction origin compared with the conduction mechanisms giving rise to the bias and temperature dependence of the forward current determined by the bulk properties of the solid rather than contact effects. Thus, an analysis of the bias and temperature dependence of the measured heterojunction reverse current on the basis of the bulk conduction model (such as SCLC) used in analysing the forward bias current behaviour is understood to give a less satisfactory interpretation of the overall high reverse bias current

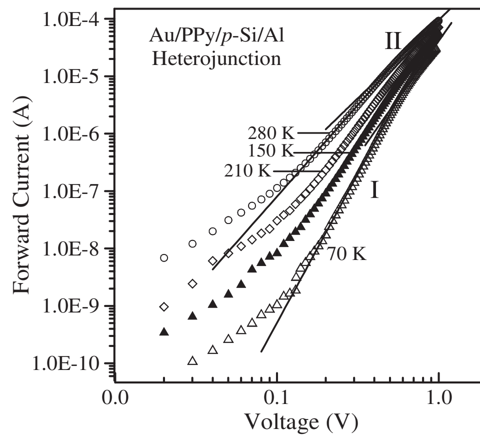

Figure 3. Experimental forward bias $\log(J)$ versus $\log(V)$ plot of the Au/PPy/p-Si/Al heterocontact at four different temperatures from the plots given in figure 1.

behaviour. Therefore, the measured high bias reverse current is more likely to be governed by the actual junction-like behaviour via the charge transport mechanisms operable in the heterojunction depletion region.

Figure 3 shows the double-logarithmic forward bias I–V plots of the Au/PPy/p-Si/Al heterojunction at four different temperatures. As is seen from figure 3, the double-logarithmic forward bias I–V plots exhibit a good linearity in the voltage range 0.2–1.0 V. At high applied voltage, the forward I–V characteristics in the temperature range 70–280 K are influenced by the transport properties of the highly resistive PPy layer [28, 29, 34]. In general, the double-logarithmic forward bias I–V plots with a slope equal to or larger than 2 suggest the possibility of the space-charge-limited current (SCLC) mechanism [29, 34–38]. The double-logarithmic forward bias I–V plots in figure 3 show a power-law behaviour of the current $I \propto V^{m+1}$ with different exponents $(m + 1)$. That is, such power laws with exponents larger than two have been interpreted as indication for trap-charge-limited conduction with an exponent trap distribution [34–36]. However, the space charge formation and the distribution nature of traps in a specimen, which often immobilize the injected charge carriers, are important factors that govern the SCLC mechanism. The SCLC conduction should become important when the density of injected free-charge carriers is much larger than the thermally generated free-charge-carrier density. In our case, the injected charge carriers can be proceed through the junction from the moderately doped p-Si ($p \sim 1.984 \times 10^{15}$ cm^{-3}) into the highly resistive PPy material with much lower concentration of free holes to sustain flow of trap charge-limited currents (TCLCs).

The trap-charge-limited current density dominated by an exponential distribution of traps in the band gap of the organic thin film is given by [29, 34–38]

$$J = q\mu N_{\mathrm{v}} \left(\frac{\varepsilon\varepsilon_0}{qN_{\mathrm{t}}}\right)^m \frac{V^{m+1}}{d^{2m+1}}, \tag{1}$$

where ε is the permittivity of the PPy and is taken as about 13.1 [10], $\varepsilon_0 = 8.85 \times 10^{-12}$ F m^{-1} is the permittivity of free space, N_{v} is the effective density of states in the valence band of the PPy, μ is mobility of holes in the PPy, $N_{\mathrm{t}} = P_0 k T_{\mathrm{c}}$ [38] is the total concentration of traps, P_0 is the trap concentration per unit energy range at the valence band edge and is expressed by $P(E) = P_0 \exp(-E/kT_{\mathrm{c}})$, $P(E)$ is the trap concentration per unit energy range at an energy E above the valence band edge, $m = T_{\mathrm{c}}/T = E_{\mathrm{t}}/kT$, T_{c} is the characteristic temperature

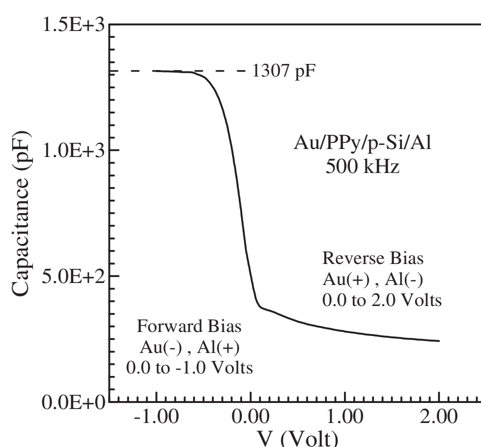

Figure 4. Experimental high-frequency capacitance–voltage plot of the Au/PPy/p-Si/Al hetero-contact at 280 K and 500 kHz.

parameter of the trap distribution, T is the ambient temperature, and d is the thickness of the PPy film. Figure 4 shows the C–V curves of the Au/PPy/p-Si/Al heterojunction at 500 kHz and 280 K. In high-frequency measurements, the measured value of the capacitance depends on the thickness of the organic PPy and inorganic p-Si layers, and it is given by $C^{-1} = C_{\mathrm{pol}}^{-1} + C_{\mathrm{Si}}^{-1}$ as expected for two layers in series, for $C_{\mathrm{traps}} = 0$ in equation (1) as in [18]. That is, when a negative voltage is applied to the Au metal plate, the capacitance increases towards high negative voltage and reaches the capacitance of the PPy layer alone. That is, the shape of the curve suggests charge accumulation at the organic/inorganic interface and thus the capacitance of the PPy layer C_{pol} becomes important [38–41]. As can be seen from the C–V curve in figure 4, the value of C_{pol} is 1307 pF. Now, we can calculate the PPy layer thickness, d, from the high-frequency (HF) C–V characteristics of the heterojunction using the equation $C_{\mathrm{pol}} = \varepsilon\varepsilon_0 A/d$. Thus, the PPy layer thickness was calculated as approximately 210 nm.

The power-law parameter, m, values were calculated from the slopes of the linear portions of the double-logarithmic I–V plots under 'forward bias' of the Au/PPy/p-Si/Al contact for each measurement temperature, in the temperature range 70–280 K (figure 3). Beyond the ohmic region, the forward bias characteristics show two distinct regions at each temperature. The value of $(m + 1)$ in region I varied from 3.25 at 280 K to 5.20 at 70 K. Figure 5 is a plot of the temperature-dependent exponent m from the power laws in the I–V characteristics versus reciprocal temperature, which is fitted by a straight line corresponding to $T_{\mathrm{c}} = 194$ K. The slopes $(m + 1)$ for region II of the I–V curves in the temperature range 70–280 K changed from 2.30 at 280 K to 4.39 at 70 K. However, according to the values of m, the temperature parameter can be calculated as $T_{\mathrm{c}} = mT = 632.8$ K for $T = 280$ K, and $T_{\mathrm{c}} = 294$ K for $T = 70$ K. As can be seen from figure 5, the exponent m seems to increase with decreasing temperature. This plot should yield a straight line through the origin. This behaviour can be used to derive the characteristic trap energy E_{t} from the temperature dependence of $kT_{\mathrm{c}} = E_{\mathrm{t}}$. According to this relation, the plot shows indeed a linear dependence with a slope yielding a trap energy value of 0.02 eV. However, the straight line does not go through the origin because the mobility of the organic layer depends on the electric field.

As can be seen from figure 6, the slope of forward current log J–$1/T$ curves decreases with increasing bias voltage, that is, the curves exhibit an electric field-dependent linearity. The value of 0.02 eV cannot be reliably interpreted as the minimum energy for a change carrier

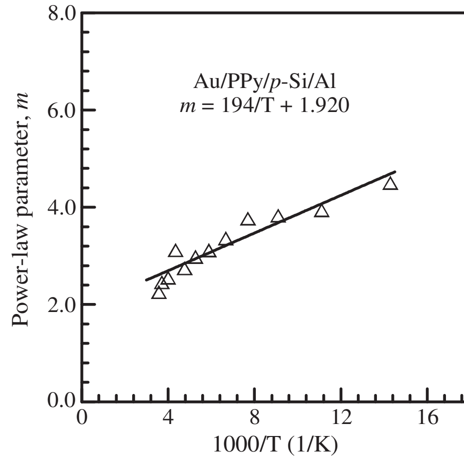

Figure 5. Power-law parameter m versus $1/T$ plot; m values were obtained from the slope of the $\log(J)$ versus $1/T$ plot corresponding to each temperature for region I.

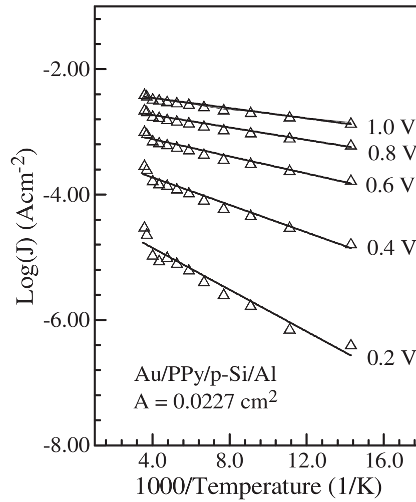

Figure 6. Experimental forward bias $\log(J)$ versus $1/T$ plot at five different voltages from figure 1 in the temperature range 70–280 K (the open triangles); the solid lines represent the fit to experimental data.

to be thermally emitted from a trap state near the Fermi level to the semiconductor energy band involved [29]. In figure 6, the open triangles show the experimental $\log(J)$ versus $1/T$ plot in the voltage range 0.20–1.00 V with steps of 0.02 V. The plots give straight lines in the temperature range 70–280 K at each voltage. As mentioned above, the slopes of forward current $\log J$–$1/T$ curves exhibit a bias voltage-dependent linearity. The slope of the line presented in the $\log(J)$ versus $1/T$ plots is given by [36, 37]

$$\frac{\mathrm{d}(\log J)}{\mathrm{d}(1/T)} = T_{\mathrm{c}} \log \frac{\varepsilon V}{q d^2 N_{\mathrm{t}}(E)}, \tag{2}$$

from which the value of $N_{\mathrm{t}}(E)$ is determined, and the intercept on the $\log(J)$ axis is written as

$$\log J_i = \log(q\mu N_{\mathrm{v}} V/d), \tag{3}$$

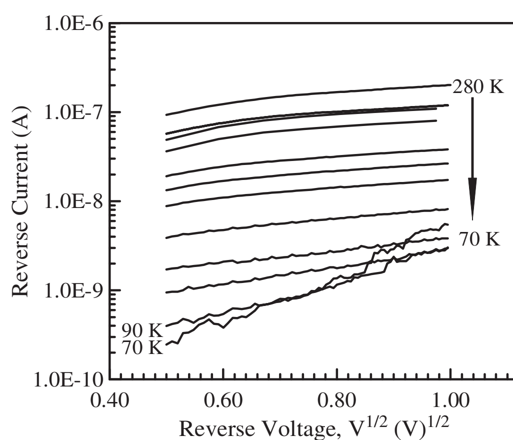

Figure 7. Experimental temperature-dependent semi-log reverse bias current versus $V^{1/2}$ plots of the Au/PPy/p-Si/Al hetero-contact.

Table 1. The experimental parameters obtained for the Au/PPy/p-Si/Al heterojunction in the temperature range 80–2800 K.

Bias voltage (V)	N_t (cm^{-3})	P_0 (cm^{-3} eV^{-1})	μ (cm^2 V^{-1} s^{-1})
0.20	2.281×10^{14}	1.363×10^{16}	8.164×10^{-5}
0.40	4.487×10^{14}	2.682×10^{16}	6.786×10^{-5}
0.60	7.299×10^{14}	4.362×10^{16}	5.959×10^{-5}
0.80	9.146×10^{14}	5.466×10^{16}	5.303×10^{-5}
1.00	1.018×10^{15}	6.082×10^{16}	4.738×10^{-5}

where J_i represents the current density at infinite temperature ($1/T = 0$) and immediately yields the mobility μ. The $\log(J)$ versus $1/T$ plot at 0.2 V curve in figure 6 has a slope of 166 A K cm^{-2} and an intercept of 0.633 A cm^{-2} in the temperature range 70–280 K. Thus, the values of $N_t = 2.281 \times 10^{14}$ cm^{-3}, $P_0 = 1.363 \times 10^{16}$ cm^{-3} eV^{-1} and $\mu = 8.164 \times 10^{-5}$ cm^2 V^{-1} s^{-1} for PPy were obtained using equations (1)–(3). The mobility value in conjugated polymers is found to be around 10^{-4} cm^2 V^{-1} s^{-1} and it is known to depend on field and temperature [42]. The obtained value for the mobility appears to be in agreement with the value of about 10^{-4} cm^2 V^{-1} s^{-1} given for polymeric thin films [42]. The parameter values corresponding to the other applied voltages in figure 6 are given in table 1.

As mentioned above, the experimental high bias reverse current given in figure 1 is more likely to be governed by the actual junction-like behaviour via the charge transport mechanisms in the heterojunction. This junction-like behaviour is clearly exemplified in the temperature-dependent semi-log reverse bias current versus $V^{1/2}$ plots, as depicted in figure 7; the linearity in the temperature-dependent semi-log reverse bias current versus $V^{1/2}$ plots can be noticed at reverse voltages above 0.3 V. In the PPy/p-Si heterojunction, this current may be understood in terms of the Schottky emission (field-lowering of the interfacial barrier at the injected electrode interface) or Poole–Frenkel effect (field-assisted thermal detrapping of carriers). The reverse bias I–V expressions for these processes are given by [29, 36, 43, 44]

$$I = I_{R0} \exp\left(\frac{\beta_S V^{1/2}}{kTd^{1/2}}\right) \qquad (4)$$

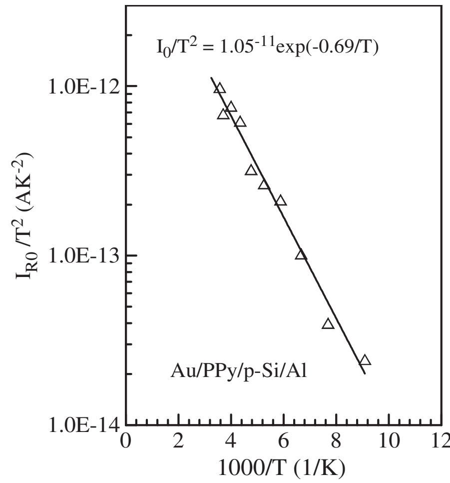

Figure 8. Reverse bias I_{R0}/T^2 versus $1/T$ plot of the Au/PPy/p-Si/Al hetero-contact.

for the Schottky effect and

$$I = I_{R0}\exp\left(\frac{\beta_{\mathrm{PF}}V^{1/2}}{kTd^{1/2}}\right) \tag{5}$$

for the Poole–Frenkel effect, where V is the bias voltage, β_{S} and β_{PF} are the Schottky and Poole–Frenkel field lowering coefficients, respectively. Theoretical values of these coefficients are given by

$$2\beta_{\mathrm{S}} = \beta_{\mathrm{PF}} = (q^3/\pi\varepsilon\varepsilon_0)^{1/2}. \tag{6}$$

This gives $\beta_{\mathrm{S}} = 1.05 \times 10^{-5}$ eV m$^{1/2}$ V$^{-1/2}$ $\beta_{\mathrm{PF}} = 2.10 \times 10^{-5}$ eV m$^{1/2}$ V$^{-1/2}$; I_{R0} is the low-field current derived from the straight line intercept of the semi-log reverse current versus $V^{1/2}$ plots, as depicted in figure 7, and it is given by

$$I_{R0} = AA^{*}T^2\exp\left(-\frac{q\Phi_{\mathrm{b}}}{kT}\right), \tag{7}$$

where q is the electron charge, A is the effective device area, k is the Boltzmann constant, T is the absolute temperature, A^{*} is the effective Richardson constant of 120 A cm^{-2} K^{-2} assuming m^{*} (the effective mass of electron) to be nearly equal to m (the mass of electron), and Φ_{bo} is the Schottky barrier height. Figure 8 shows the reverse bias I_{R0}/T^2 versus $1/T$ plot, that is, the temperature dependence of I_{R0} for the reverse current. The barrier height Φ_{b} was also evaluated for the sample using equation (7) at each temperature and the Φ_{b} versus T plot is given in figure 9. A linear temperature dependence of Φ_{b} was observed. The barrier height value ranged from 0.69 eV at 280 K to 0.22 eV at 70 K. Furthermore, an experimental value of 3.82×10^{-5} eV m$^{1/2}$ V$^{-1/2}$ for β was obtained from the slope of the graph plotted between the reverse bias $\ln J$ and $V^{1/2}$ at 280 K. The experimental value of β is compared with the theoretical values of the PPy, $\beta_{\mathrm{S}} = 1.05 \times 10^{-5}$ eV m$^{1/2}$ V$^{-1/2}$ $\beta_{\mathrm{PF}} = 2.10 \times 10^{-5}$ eV m$^{1/2}$ V$^{-1/2}$ given above. The experimental value of 3.82×10^{-5} eV m$^{1/2}$ V$^{-1/2}$ is in close agreement with the experimental value of 2×10^{-5} eV m$^{1/2}$ V$^{-1/2}$ for PPy given by Kumar *et al* [44].

In conclusion, a rectifying contact was formed between p-Si and gold by means of the interfacial PPy layer because generally the junctions between p-Si and metals such as gold or

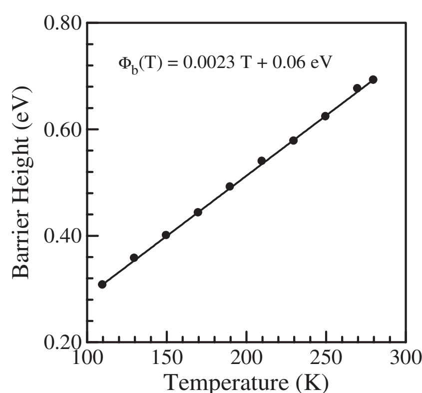

Figure 9. Temperature-dependent barrier height plot of the Au/PPy/p-Si/Al hetero-contact.

aluminium are expected to form an ohmic contact; and the bulk parameters of the PPy film, that is a good candidate for the active part of electronic devices, were calculated. The forward bias I–V characteristics of the polymeric organic compound polypyrrole (PPy) interfaced to the inorganic p-Si have been explained by using the space-charge-limited current (SCLC) density model dominated by exponential distribution of traps. The values of $N_t = 2.281 \times 10^{14}$ cm^{-3}, $P_0 = 1.363 \times 10^{16}$ cm^{-3} eV^{-1} and $\mu = 8.164 \times 10^{-5}$ cm^2 V^{-1} s^{-1} for the PPy layer were obtained from the forward bias $\log(J)$ versus $1/T$ plots at temperatures ranging from 70 to 280 K. The temperature dependences of the barrier height values from the experimental reverse bias I–V characteristics interpreted by the Schottky or Poole–Frenkel effect models have been seen to be linear.

References

[1] Abthagir P S and Saraswathi R 2004 *J. Mater. Sci., Mater. Electron.* **15** 81
[2] Liang G R, Cui T H and Varahramyan K 2003 *Microelectron. Eng.* **65** 279
Liang G R, Cui T H and Varahramyan K 2003 *Solid-State Electron.* **47** 691
[3] Lonergan M 2004 *Annu. Rev. Phys. Chem.* **55** 257
Lonergan M C 1997 *Science* **278** 2103
[4] Gök A and Sari B 2002 *J. Appl. Polym. Sci.* **84** 1993
[5] Migahed M D, Fahmy T, Ishra M and Barakat A 2004 *Polym. Test.* **23** 361
[6] Yamamoto T, Wakayama H, Fukuda T and Kanbara T 1992 *J. Phys. Chem.* **96** 8677
Yamamoto T, Kanbara T, Mori C, Wakayama H, Fukuda T, Inone T and Sasaki S 1996 *J. Phys. Chem.* **100** 12631
[7] El-Sayed S M, Hamid H M A and Radwan R M 2004 *Radiat. Phys. Chem.* **69** 339
[8] Forrest S R 1997 *Chem. Rev.* **97** 1793–896
[9] Ishii H, Sugiyama K, Ito E and Seki K 1999 *Adv. Mater.* **11** 605
[10] Nguyen V C and Kamloth K P 2000 *J. Phys. D: Appl. Phys.* **33** 2230
[11] Kamloth K P 2002 *Crit. Rev. Anal. Chem.* **32** 121
[12] Nguyen V C and Kamloth K P 1999 *Thin Solid Films* **338** 142
[13] Singh R and Narula A K 1997 *Appl. Phys. Lett.* **71** 2845
[14] Bozkurt A, Akbulut U and Toppare L 1996 *Synth. Met.* **82** 41
[15] Bozkurt A, Ercelebi C and Toppare L 1997 *Synth. Met.* **87** 219
[16] Aydoğan Ş, Sağlam M and Türüt A 2005 *Vacuum* **77** 269
Aydoğan Ş, Sağlam M and Türüt A 2005 *Polymer* **46** 563
Aydoğan Ş, Sağlam M and Türüt A 2005 *Synth. Met.* **150** 15
Aydoğan Ş, Sağlam M and Türüt A 2005 *Synth. Met.* **87** 15
Aydoğan Ş, Sağlam M and Türüt A 2005 *Appl. Surf. Sci.* **250** 43
[17] Vermeir I E, Kim N Y and Laibinis P E 1999 *Appl. Phys. Lett.* **74** 3860

[18] Musa I and Eccleston W 1999 *Thin Solid Films* **343/344** 469
[19] Çakar M, Temirici C and Türüt A 2004 *Synth. Met.* **142** 177
[20] Roberts A R V and Evans D A 2005 *Appl. Phys. Lett.* **86** 072105
[21] Zhao J and Uosaki K 2004 *J. Phys. Chem.* B **108** 17129
[22] Horvath Z J, Adam M, Godio P, Borionetti G, Szabo I, Gombia E and Van Tuyen V 2002 *Solid State Phenom.* **82–84** 255
Horváth Zs J, Ádám M, Szabó I, Serényi M and Van Tuyen V 2002 *Appl. Surf. Sci.* **190** 441
[23] Sehgal B K, Balakrishnan V R and Gulati R 2003 *J. Semicond. Technol. Sci.* **3** 1–12
[24] Ebeoğlu M A, Temurtaş F T and Öztürk Z Z 1998 *Solid-State Electron.* **42** 23
[25] Lu X, Xu X, Wang N Q, Zhang Q and Lin M C 2001 *J. Phys. Chem.* B **105** 10069
Lu X and Lin M C 2002 *Int. Rev. Phys. Chem.* **21** 137
[26] Hanselaer P L, Lafléré W H, Van Meirhaeghe R L and Cardon F 1986 *Appl. Phys.* A **39** 129
[27] Dakhel A A 2004 *J. Alloys Compounds* **376** 38
[28] Kassim A, Basar Z B and Mahmud H N M E 2002 *Proc. Indian Acad. Sci. Chem. Sci.* **144** 155
[29] Jafar M M A 2003 *Semicond. Sci. Technol.* **18** 7
[30] Assadi A, Spetz A, Willander M, Svensson C, Lundström I and Inganäs O 1994 *Sensors Actuators* B **20** 71
[31] Bott B and Thorpe S C 1991 *Techniques and Mechanism in Gas Sensing* (*Adam Hilger Series on Sensors*) ed P T Moseley, J Norris and D E Williams (Philadelphia, PA: IOP Publishing) chapter 5, p 139
[32] Hanawa T, Kuwabata S and Yoneyama H 1988 *J. Chem. Soc. Faraday Trans.* **84** 1587
[33] Shen Y and Wan M 1998 *Synth. Met.* **98** 147
[34] Abdel-Malik T G and Abdel-latif R M 1997 *Thin Solid Films* **305** 336
[35] Lampert M A 1964 *Rep. Prog. Phys.* **27** 329
[36] Anthopoulos T D and Shafai T S 2003 *J. Phys. Chem. Solids* **64** 1217
Shafai T S and Anthopoulos T D 2001 *Thin Solid Films* **398/399** 361
[37] Gould R G 1986 *J. Phys. D: Appl. Phys.* **9** 1785
Gould R G and Rahman M S 1981 *J. Phys. D: Appl. Phys.* **14** 79
[38] Brutting W, Berleb S and Muckl A G 2001 *Org. Electron.* **2** 1–36
[39] Nicollian E H and Goetzberger A 1967 *Bell. Syst. Tech.* **46** 1055
[40] Chattopadhyay P and RayChaudhuri B 1993 *Solid-State Electron.* **36** 605
[41] Biber M, Cakar M and Turut A 2001 *J. Mater. Sci. Mater. Electron.* **12** 575
[42] Leising G, Tasch S and Graupner W 1998 *Handbook of Conducting Polymers* 2nd edn, ed T A Skotheim, R L Elsenbaumer and J R Reynolds (New York: Dekker) p 862
[43] Simmons J G 1971 *J. Phys. D: Appl. Phys.* **4** 613
[44] Kumar D S, Nakamura K, Nishiyama S, Ishii S, Noguchi H, Kashiwagi K and Yoshida Y 2003 *J. Appl. Phys.* **93** 2705